

# Out-of-Band Emissions of Digital Transmissions Using Kahn EER Technique

Dietmar Rudolph

**Abstract**—The Kahn envelope elimination and restoration (EER) technique allows for linear RF power amplification by combining nonlinear, but efficient, RF and AF power amplifiers (PAs). In order to use the EER technique for digital signals, a coordinate transform from the original Cartesian in-phase and quadrature mode into a polar mode has to take place, yielding an envelope (or amplitude) and a PM RF signal. This coordinate transform is extremely nonlinear and thereby broadens the spectra of the original signals. In the final PA stage, both signals are recombined. However, since this recombination process is imperfect, out-of-band (OOB) emissions come up, also known as adjacent channel power or spectral regrowth. In this paper, the impact of the broadening of the amplitude and phase signals on OOB emissions is investigated with respect to imperfect restoration due to signal delays and limited bandwidth of the amplitude path. It is shown that the amount of OOB emissions can significantly be reduced if the modulation scheme shows a “hole” at the origin in its vector diagram.

**Index Terms**—ACPR, amplifier, band-limited communications, delay effects, EER, Kahn technique, PM, spectral regrowth, transmitter.

## I. INTRODUCTION

DIGITAL cellular transmission systems, as well as digital broadcasting systems, widely use modulation formats that do not have a constant envelope, e.g.,  $\pi/4$ DQPSK, OQPSK, and additionally with zero crossings in their vector diagram, e.g., QPSK, eight phase shift keying (8PSK), amplitude phase shift keying (APSK), orthogonal frequency division multiplex (OFDM), CDMA. If the amplitude of the digitally modulated signal is not constant, the transmitter power amplifier (PA) has to operate in linear mode. Linear operation mode can either be established by a linear amplifier, which suffers from low efficiency [2], or by a transmitter that linearizes a high-efficiency PA, e.g., by using the envelope elimination and restoration (EER) technique proposed by Kahn in 1952 [1]–[11]. In an EER transmitter, basically, the RF signal is split into a PM and an AM signal. The PM signal is directly amplified by a PA that runs in a saturated or even switching mode. In order to restore the amplitude, the supply voltage of the PA is modulated by the AM signal. Thereby, although the PA itself is operated in a nonlinear high-efficiency mode, the total transmitter shows linear behavior while maintaining the high efficiency. The benefits of the EER technique with respect to the transmitter’s efficiency are without any question. The EER technique, however, introduces a coordinate transform of the digital signal from

Cartesian to polar form, and the PA stage of an EER transmitter afterwards produces the inverse coordinate transform back. In this way, linear distortions within the “polar” branches of the transmitter are transformed back into nonlinear distortions in the RF signal, even if the transmitter itself had no additional hardware nonlinearities. The coordinate transformation process is an additional extreme nonlinearity within the transmission chain. Therefore, the EER technique also has its drawbacks, which are the out-of-band (OOB) emissions.

For the case of an analog two-tone signal, Raab [6] has analyzed the intermodulation distortion (IMD) spectra. In this paper, however, the investigation is limited to the effects produced by the additional EER nonlinearities. As a signal, a band-limited complex Gaussian noise is used. This signal is very similar to an OFDM modulation. With respect to its vector diagram, it has a maximum of zero crossings, and might be in so far together with its high Crest factor the worst case of all digital modulations for EER transmitters. Based on numerical simulations, this paper first examines the broadening of the internal phase and amplitude spectra with respect to the modulation scheme. The influence of unequal time delay in the amplitude and phase branch on OOB emissions and the required bandwidth of both branches are then discussed. It turns out that a “hole” in the vector diagram of the modulation scheme significantly reduces the OOB emissions.

As a result, the amount of unwanted emissions depends on the type of digital modulation used. A modulation scheme that already has such a “hole,” like digital offset modulations, is better suited for EER techniques than others. Also, the bigger the “hole,” the better.

## II. CARTESIAN-TO-POLAR CONVERSION

The structure of a transmitter using EER is shown in Fig. 1. It is subdivided into two building blocks, i.e., the digital modulator and AM transmitter. In the digital modulator, the signal is split into a phase signal (RF-P) and an amplitude (A) signal, which serve as the input signals of the AM transmitter. The digital signal (“Digital Signal”) at the input of the modulator shall already describe the transmit symbols, and all coding shall have been done in stages prior to the digital modulator, not shown in Fig. 1. In the first step, the digital modulator forms in-phase and quadrature (I & Q) symbols, consisting of I & Q baseband symbols, and shapes them properly. The spectra of these digital signals are band limited to half the channel bandwidth and have shoulder distances of approximately 70 dB. When modulated, they fit exactly into the channel bandwidth. These Cartesian I & Q signals are then converted into polar RF-P & A signals. This process introduces the nonlinearity that is typical for EER

Manuscript received August 15, 2001.

The author is with T-Systems Nova GmbH, Berkom, D-10589 Berlin, Germany (e-mail: dietmar.rudolph@t-systems.de).

Publisher Item Identifier 10.1109/TMTT.2002.801349.

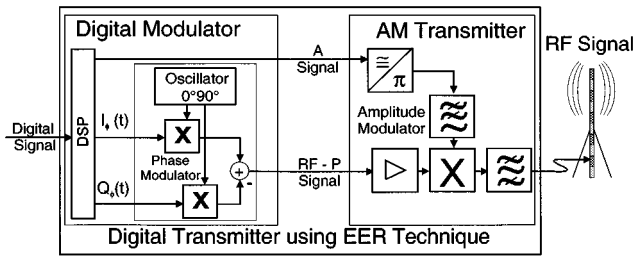


Fig. 1. Structure of an EER transmitter.

techniques. The AM transmitter has a conventional structure. The RF path is a chain of RF driver and RF power output stage, both operating in classes C, D, E, or F, respectively, with high efficiency. The PA receives its supply voltage via an amplitude modulator, which operates in class S, switched mode. A partial drive modulation to overcome amplitude-to-phase (A/Phi) conversions in the PA, suggested by Raab [8], is also possible, but is not shown in Fig. 1. In this paper, the modulation process in the PA is idealized and, thus, does not suffer from A/Phi conversions.

In the EER application, the I & Q symbols are only internal Cartesian signals, which have to be converted to polar signals. According to Fig. 1, the conversion to polar signals is done all digitally in the following way. Generating a  $\varphi(t)$  signal explicitly is avoided because the phase angle is not limited, and an overflow could happen. Alternatively, two signals  $I_\varphi = \cos(\varphi(t))$  and  $Q_\varphi = \sin(\varphi(t))$  are used, which are confined to  $\pm 1$ .

The  $I_\varphi$  component is multiplied by  $\cos(\omega_C t)$  and the  $Q_\varphi$  component is multiplied by  $\sin(\omega_C t)$ , and  $\omega_C$  is the RF carrier frequency.

When using “Cartesian” I & Q signals, the complex digital-modulated signal  $s_D$  becomes

$$s_D(t) = I(t) \cdot \cos(\omega_C t) + j \cdot Q(t) \cdot \sin(\omega_C t). \quad (1)$$

The EER technique has to furnish the same digitally modulated signal  $s_D$  at the transmitter’s output.

Amplitude  $A(t)$  and phase  $\varphi(t)$  signals, used for exciting the AM transmitter, are “polar” signals, and we get

$$A(t) = \sqrt{I(t)^2 + Q(t)^2} \quad (2)$$

$$\varphi(t) = \arctan \frac{-Q(t)}{I(t)} \quad (\text{internal signal})$$

$$I_\varphi(t) = \cos(\varphi(t)) \quad (3)$$

$$Q_\varphi(t) = \sin(\varphi(t)). \quad (4)$$

Since the coordinate transform Cartesian to polar is highly nonlinear, the  $A(t)$  and  $\varphi(t)$  signals, as well as the  $I_\varphi(t)$  and  $Q_\varphi(t)$  signals, have a much broader spectra than the  $I(t)$  and  $Q(t)$  signals.

According to Fig. 1, the PM RF signal (i.e., RF-P signal)  $s_{\text{RF-P}}(t)$  becomes

$$\begin{aligned} s_{\text{RF-P}}(t) &= \cos(\varphi(t)) \cos(\omega_C t) - \sin(\varphi(t)) \sin(\omega_C t) \\ &= \cos(\omega_C t + \varphi(t)). \end{aligned} \quad (5)$$

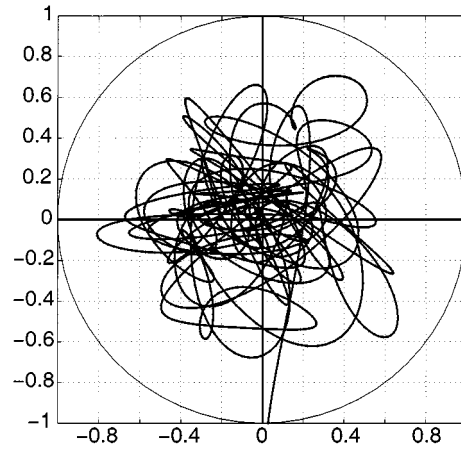


Fig. 2. Example of vector diagram of I & Q noise signal.

Thus, the RF-P signal  $s_{\text{RF-P}}(t)$  is a purely PM signal.

The PA stage of the AM transmitter operates in principle as a multiplier. This is indicated by a letter “X” in the PA block, and gives the output signal

$$s_D(t) = A(t) \cdot s_{\text{RF-P}}(t) \quad (6)$$

$$s_D(t) = A(t) \cdot \text{Re} \left\{ e^{j\varphi(t)} \cdot e^{j\omega_C t} \right\} \quad (7)$$

$$s_D(t) = I(t) \cos(\omega_C t) + j \cdot Q(t) \sin(\omega_C t). \quad (8)$$

For convenience, the amplification is set to one, and the time functions  $s_D(t)$  are equal again, thus, the spectra are the same. The TX internal broad-band spectra are compensated and no longer appear in the output signal  $s_D(t)$  of the TX. That is the ideal case.

### III. SPECTRA OF SIGNALS IN AN EER TRANSMITTER

The characteristic spectral features of the polar A and RF-P signals can most clearly be shown with band-limited Gaussian-noise-like signals, which have a Rayleigh amplitude distribution function.

All spectra in this paper are calculated with MATLAB. For convenience, the axes in the figures are normalized with respect to the bandwidth of the noise, and the amplitudes are also normalized to one.

The zero approaches of the A signal correspond to respective approaches to the origin in the vector diagram of the I & Q signals (Fig. 2). These cause rapid changes in the phase angle and, in turn, corresponding frequency deviations, leading to the peaks shown in Fig. 3.

However, wedges or cusps of the A signal and rapid phase changes or even phase jumps of the  $\varphi$  signal produce broad spectra of either these signals, and also of the RF-P signal. Also, the broader the spectra are, the worse the compensation in the PA stage becomes and the more OOB emission comes up. Thus, a straightforward idea to avoid all those problems is to “punch a hole” into the vector diagram, provided that the modulation scheme does not have it as before, as in the case of OFDM.

Fig. 4 shows spectra of the I & Q signals and the A signal. The curve labeled “without Vector Hole” shows the actual spectrum. The curve labeled “with Vector Hole” indicates a method as to

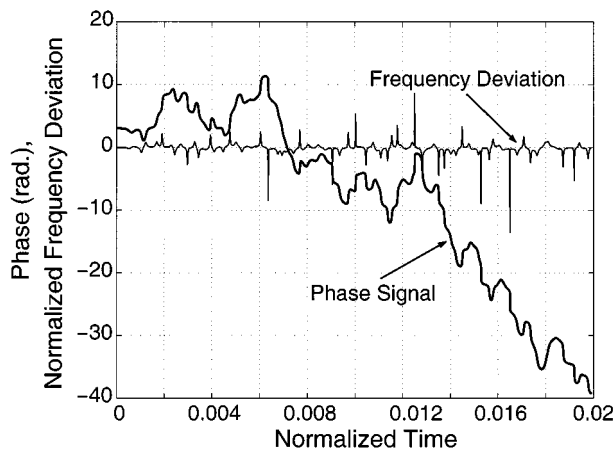


Fig. 3. Phase and frequency deviations of the I & Q noise signal.

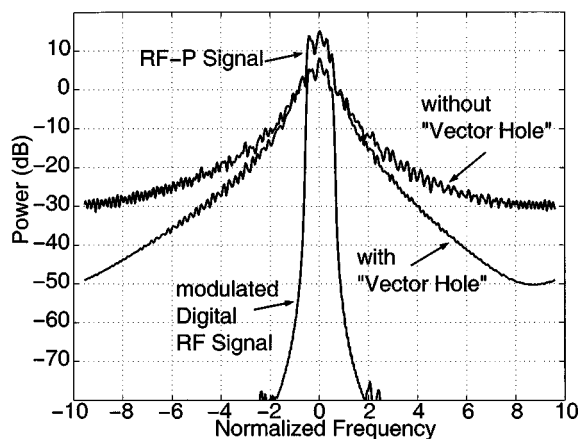


Fig. 5. Spectra of the RF-P and the modulated digital RF signal.

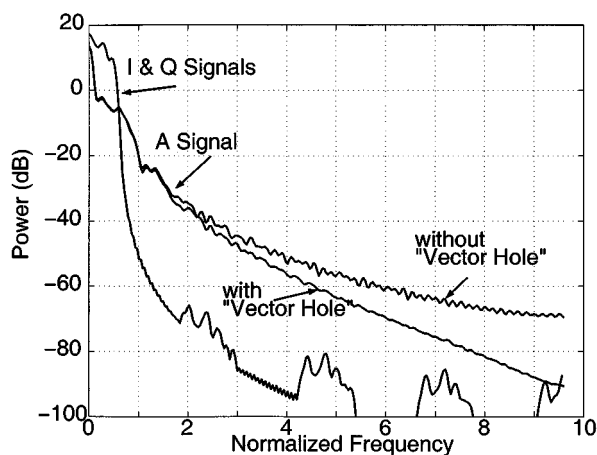


Fig. 4. Spectra of the I & Q and A signals.

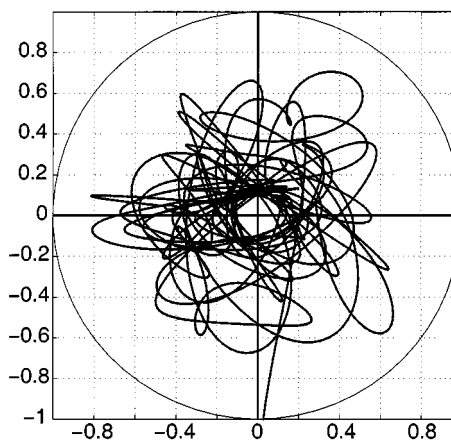


Fig. 6. Example of vector diagram of complex noise with a "hole."

how to overcome the problem for noise-like signals, and will be discussed below.

In Fig. 5, the spectra of the modulated digital and RF-P signals are shown. The actual spectrum is again labeled "without Vector Hole."

#### IV. SOFT CLIPPING OF THE A SIGNAL

For noise-like signals, the A signal will be clipped, usually at its top in order to reduce the Crest factor of the modulated signal. This is a well-known practice to yield higher output signals of a transmitter. In this approach, the clipping will be done at the lower end of the A signal, in order to prevent zero crossings. First, a clipping threshold is defined, which, here, for convenience, is 10% of the maximum of the A signal. The amount of the A signal beneath this threshold defines a clipping signal. This clipping signal is shaped Gaussian in order to fit spectrally into the signal bandwidth. Afterwards, it is then added vectorially to the I & Q signal and, thus, "punches a hole" into the vector diagram (Fig. 6). This kind of "soft clipping" avoids spectral splatter.

Fig. 7 shows the A signal and clipping threshold together with the soft clipping signal. The time positions of the latter signal correspond to the frequency peaks in Fig. 3.

Fig. 5 shows the improvement in the spectrum of the RF-P signal by "punching or drilling a hole" into the vector diagram. The improvement in the A signal is similar. All spectral components now attenuated within these signals are no doubt more easily compensated in the PA stage of the transmitter.

It is beyond the scope of this investigation as to how big the hole might become regarding the increase of the bit error rate of the digital transmission. However, it is evident that modulation schemes that already provide a "vector hole" will better fit to an EER transmitter. Also, it is known from AM transmitters that they do have difficulties with attaining a real zero in their envelope signal. A method to mitigate this problem is a partial drive modulation [8], which is unfortunately not applicable to all types of AM transmitters.

The greater the "hole" in the vector diagram of a given modulation scheme, the steeper the slope in the spectra of the A and RF-P signals will become. Fig. 8 shows simulation results, depending on the radius of the hole in percent of the maximum vector diagram radius, which is normalized to one. Without a hole, the slopes for the RF-P signal are only -3.5 dB and for the A signal are only -9.5 dB within a frequency range equal to the RF bandwidth. Note that all figures given are normalized to the RF bandwidth.

A modulation scheme with a hole in the vector diagram greatly improves the slopes of both signals.

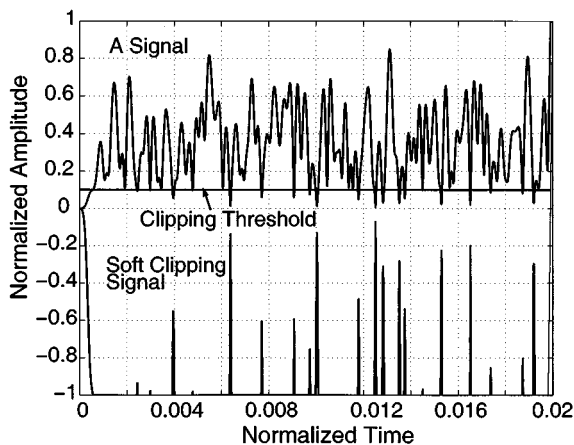


Fig. 7. A signal, clipping threshold, and soft clipping signal.

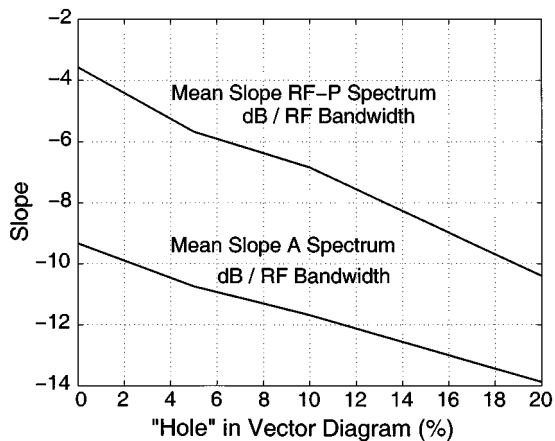


Fig. 8. Slopes of A and RF-P signals as a function of the radius of the hole in the vector diagram.

## V. DELAY AND BANDWIDTH WITHIN AN EER TRANSMITTER

After analyzing the spectra of the A and RF-P paths separately, the impact of nonideal signal restoration on the OOB emissions will be discussed here. Signal delay and bandwidth limitations of the two signals will be considered.

### A. Influence of the Delay on the OOB Emissions

In this section, the bandwidths are taken sufficiently broad, and all effects to the OOB emissions will come from delay mismatch only.

First, the case without a “vector hole” is regarded. The A signal has been delayed by  $0, T_s, 2T_s, 4T_s, 8T_s$ , i.e., in a progressive order.  $F_s = 1/T_s$  is the clock frequency used in the simulation, and is about ten times the RF bandwidth  $B_{RF}$ , thus,  $Delay = (0, 1, 2, 4, 8)/10B_{RF}$ . Fig. 9 shows that this clock frequency is too coarse for delay fine tuning and, in a practical case, upsampling has to take place. To extrapolate to smaller delays, the progressive order has to be taken into consideration. Therefore, approximately 5 dB more shoulder distance is gained if the delay is halved again, and so forth.

Something very important can be seen from this figure, as noted below.

- If the delay is unequal to zero, the spectrum of the digital signal becomes similar to the spectrum of corresponding

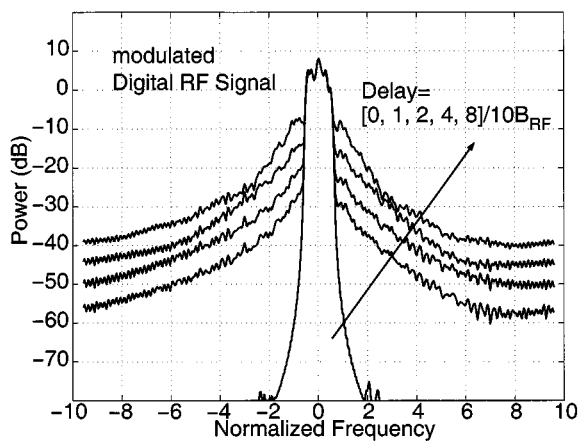


Fig. 9. Spectra of the modulated digital RF signal for various delays (without a vector hole).

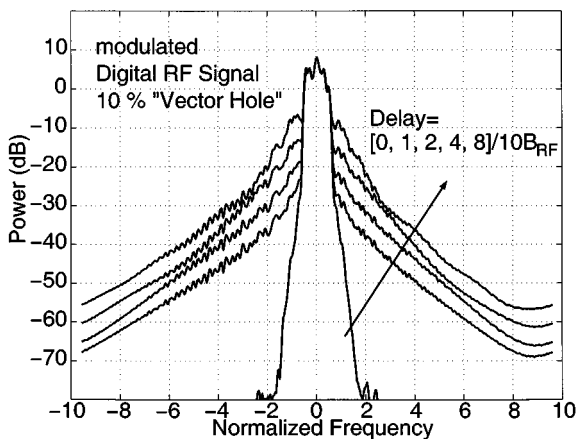


Fig. 10. Spectra of the modulated digital RF signal for various delays (with a 10% vector hole).

the RF-P signal, and the slope of the OOB is identical to the slope of the RF-P signal (see Fig. 5). For smaller delays, the shoulder becomes higher and, for big delays, in this example,  $T_d \geq 8/10B_{RF}$ , the spectrum of the digital signal is more or less identical to the spectrum of the RF-P signal. This should be kept in mind when aligning an EER transmitter for minimum OOB because, for big delays, there is hardly any difference between the RF-P spectrum and the spectrum of the digitally modulated signal. The same interrelation holds also for signals with a “vector hole” (Fig. 10), even though steeper slopes result.

- “Punching a hole” into the vector diagram only gives an improvement in the slope of the OOB emissions, but gives no improvement to the shoulder distance.
- Each doubling of the delay reduces the shoulder distance in the spectrum of the modulated digital RF signal approximately by the same amount in decibels. Therefore, delay matching has to be done very precisely.

### B. Bandwidth of the A and RF-P Paths

The RF-P path is considered first. Here,  $LC$  circuits are usually included, which give limited bandwidth. However, because the following stages in the RF path operate in class C or the like, the AM of RF-P phase signal introduced by the  $LC$  filtering is

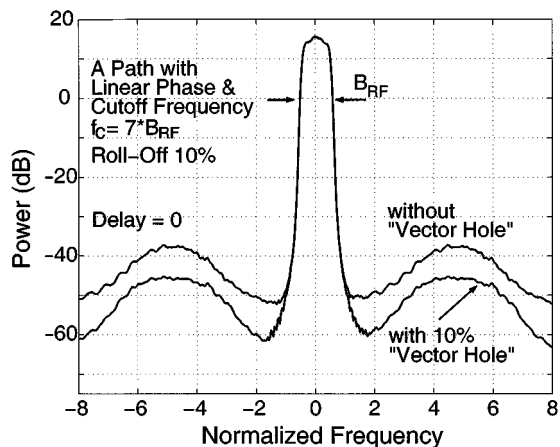


Fig. 11. Spectra of the digital signal: cutoff frequency of a path seven times the RF bandwidth.

removed, and the RF-P phase signal is restored again. This is an effect similar to the filter-limiter operation in a FM receiver, from where it is known that this works well. Therefore, the bandwidth limitation in the RF path plays no role.

From the previous section, it is clear that the delay has to be compensated very precisely. If the bandwidth limitations of the A path in the EER transmitter is now considered, we will be confined to low-pass filters with linear phase and constant group delay. Filters with nonlinear phase do not have a constant group delay and, therefore, the delay compensation cannot be done uniquely. In such cases, there will be a region of delay values where a peak in the OOB can be shifted in the frequency. In one case, the shoulder distance improves, but far off, the OOB spectrum becomes worse and vice versa. Therefore, it is necessary to have an A path with linear phase, which can be done by equalizing techniques.

As an example, the transfer function of the A path is taken as being constant to a cutoff frequency  $f_c = 7 \cdot B_{RF}$  with a rolloff factor of 10%. The phase of the A path is linear, thus, its group delay is constant. Fig. 11 shows the resulting spectra of the digital signals without and with a "vector hole," respectively.

As a rule-of-thumb, the results from simulations comparable to the example given in Fig. 11 can be interpreted as follows.

- The results only hold for delay = 0.
- The shoulder distances correspond approximately to the level of the A signals given in Fig. 4 at the frequency  $f_c = 7 \cdot B_{RF}$ .
- The improvement by a "vector hole" is less than the difference of the A signal spectra in Fig. 4.
- A peak of the OOB occurs with a relative height independent from the size of the "vector hole." This somewhat resembles the Gibb's phenomena, and there is also some resemblance to a result given by Raab [6].
- For smaller cutoff frequencies, the OOB peaks are only minor shifted to the main spectrum, but the shoulder dis-

tance becomes lower, and the valley between the main spectrum and peaks is eventually filled in.

## VI. CONCLUSIONS

For Kahn EER transmitter techniques, the OOB slope depends on the modulation used. Digital modulations that omit the origin in their vector diagram give steeper slopes. The steepness increases with the diameter of this "vector hole." In transmitter alignment, the delay between the amplitude path and RF path has to be as perfect as possible. Even a small mismatch gives a slope of the OOB identical to the slope of the PM RF (i.e., RF-P) signal and, for greater delays, the spectrum of the digital signal is practically identical with the spectrum of an RF-P signal. The transfer function of the amplitude path should have a constant amount and group delay.

## REFERENCES

- [1] L. R. Kahn, "Single sideband transmission by envelope elimination and restoration," *Proc. IRE*, vol. 40, pp. 803–806, July 1952.
- [2] W. Liu, J. Lau, and R. Cheng, "Considerations on applying OFDM in a highly efficient power amplifier," *IEEE Trans. Circuits Syst. II*, vol. 46, pp. 1329–1336, Nov. 1999.
- [3] M. Meinzer, "Lineare Nachrichtentransponder durch Signalzerlegung," Doctoral dissertation (in German), Dept. Phys., Univ. Marburg, Marburg, Germany, 1973.
- [4] —, "A linear transponder for amateur radio satellites," *VHF Commun.*, vol. 7, pp. 42–57, Jan. 1975.
- [5] M. Weiss, F. H. Raab, and Z. B. Popović, "Linearity of X-band class-F power amplifiers in high-efficiency transmitters," *IEEE Trans. Microwave Theory Tech.*, vol. 49, pp. 1174–1179, June 2001.
- [6] F. H. Raab, "Intermodulation distortion in Kahn-technique transmitters," *IEEE Trans. Microwave Theory Tech.*, vol. 44, pp. 2273–2278, Dec. 1996.
- [7] F. H. Raab, B. E. Sigmon, R. G. Myers, and R. M. Jackson, "High efficiency L-band Kahn-technique transmitter," *IEEE Trans. Microwave Theory Tech.*, vol. 46, pp. 290–292, Dec. 1998.
- [8] F. H. Raab, "Drive modulation in Kahn-technique transmitters," in *IEEE MTT-S Int. Microwave Symp. Dig.*, vol. 2, June 1999, pp. 811–814.
- [9] P. Kenington, "Linearization in base-station equipment," presented at the IEEE MTT-S Int. Microwave Symp. Workshop, June 2000.
- [10] D. Rudolph, "Principles and proposals for digital radio broadcasting systems using long, medium and shortwaves," presented at the ITG Radio Broadcasting Session, Mannheim, Germany, 1995.
- [11] —, "The DTAG ZRA digital AM system," presented at the NAB Conv.: Progress Toward Develop. Digital Modulation Longwave, Mediumwave, Shortwave Bands, 1997.



**Dietmar Rudolph** was born in Heilbronn, Germany, in 1941. He received the Dipl.-Ing. and Dr.-Ing. degrees from the Technische Universität Stuttgart, Stuttgart, Germany, in 1966 and 1972, respectively.

In 1972, he became a Lecturer, and in 1979, became a Full Professor of communication techniques with the Fachhochschule of Deutsche Bundespost, University of Applied Sciences, Berlin, Germany. In 1996, he joined the Deutsche Telekom Broadcasting Division, University of Applied Sciences. He is currently with T-Systems Nova GmbH, Berkom, Germany. He holds several patents on digital and analog broadcasting issues. His research areas include digitalization of AM broadcast and EER techniques.